Miner Deposita (2008) 43:449–466
DOI 10.1007/s00126-008-0176-4

ARTICLE

Facies analyses and volcanic setting of the giant Neves Corvo massive sulfide deposit, Iberian Pyrite Belt, Portugal

Carlos J. P. Rosa · Jocelyn McPhie · Jorge M. R. S. Relvas · Zélia Pereira · Tomás Oliveira · Nelson Pacheco

Received: 22 May 2007 / Accepted: 22 December 2007 / Published online: 9 February 2008

Abstract In the Iberian Pyrite Belt, volcanic rocks are relatively scarce, accounting for approximately only 25% of the geologic record, with the remaining 75% consisting of sedimentary units. This association is very clear in the host succession to the Neves Corvo massive sulfide deposit in Portugal. The Neves Corvo host succession comprises the products of explosive and effusive rhyolitic eruptions intercalated with mudstone that records a submarine below-wave-base environment and provides precise biostratigraphic age constraints. The first and second volcanic events involved eruptions at local intrabasinal vents. The first event generated thick beds of fiamme breccia that are late Famennian in age. The fiamme were originally pumice clasts produced by explosive eruptions and were subsequently compacted. The second event was the late Strunian (latest Famennian) effusion of rhyolitic lava that was pervasively quench-fragmented. The third and final event is younger than the massive sulfide deposits poorly represented in the mine area and minor compared with the two other events. The integration of biostratigraphic data with the volcanic facies architecture indicates that the Neves Corvo ore deposits are similar in age to the late Strunian rhyolitic lava. Although regionally the Iberian Pyrite Belt is essentially a sedimentary succession, ore formation at Neves Corvo can be closely linked to discrete volcanic events that produced a relatively narrow range of volcanic facies.

Keywords Neves Corvo, Iberian Pyrite Belt · Portugal, Massive sulfide mineralization

Editorial handling: B. Lehmann

C. J. P. Rosa · J. McPhie
CODES, ARC Centre of Excellence in Ore Deposits,
University of Tasmania,
Private Bag 79,
Hobart, Tasmania 7001, Australia

C. J. P. Rosa · J. M. R. S. Relvas
CREMINER/Dept. Geologia, Faculdade de Ciências,
Universidade de Lisboa,
Edifício C6, Piso 4, Campo Grande,
1749-016 Lisboa, Portugal

Z. Pereira
INETI, Dept. Geologia, Rua da Amieira,
Apartado 1089,
4466-956 S. Mamede de Infesta, Portugal

T. Oliveira
INETI, Dept. Geologia, Estrada da Portela, Zambujal-Alfragide,
Apartado 7586,
2720-866 Amadora, Portugal

N. Pacheco
SOMINCOR, Soc. Mineira de Neves-Corvo, S.A.,
Mina de Neves-Corvo,
7780 Castro Verde, Portugal

Present address:
C. J. P. Rosa (✉)
INETI, Dept. Prospecção Minérios Metálicos, Estrada da Portela,
Zambujal-Alfragide,
Apartado 7586,
2720-866 Amadora, Portugal
e-mail: carlos.rosa@ineti.pt

Introduction

Reconstruction of volcanic and sedimentary facies architecture has proven to be a powerful tool in understanding the stratigraphy and structure of ancient mineralized volcanic successions and in constraining massive sulfide depositional environments (e.g., Cambrian Mount Read Volcanics, Tasmania, Australia, McPhie and Allen 1992, 2003; Cambro-Ordovician Mount Windsor Subprovince, Queensland, Australia, Doyle and McPhie 2000; Proterozoic Skellefte district, Sweden, Allen et al. 1996; Ordovician Bathurst Mining Camp, Canada, Rogers et al. 2003; Archaean Noranda district, Canada, Gibson and Watkinson 1990). The Iberian Pyrite Belt (IPB) is distinctive among volcanic-hosted massive sulfide (VHMS) provinces in comprising abundant sedimentary units, and only few volcanic units, and in the large size of the ore bodies (Tornos 2006). Although sedimentary units are predominant, the massive sulfide ore bodies, including five giant deposits with more than 100 Mt, are associated with felsic volcanic rocks and black mudstone. Studies of the physical volcanology and volcanic facies architecture in the IPB have only recently been done in some detail (Boulter 1993a, b, 1996, 2002; Boulter et al. 2001, 2004; Soriano and Marti 1999; Donaire et al. 2002; Valenzuela et al. 2002), and there have been no previous studies of the host succession of the Neves Corvo deposit, one of the largest and richest deposits of the IPB. Neves Corvo contains more than 300 Mt of sulfides, of which, 100 Mt contain 3.46% Cu and 3.54% Zn, and 50 Mt contain ~6% Zn (Relvas et al. 2002, 2006a). The extremely high copper grade and presence of about 300, 000 t of tin metal mainly in the form of cassiterite and stannite make Neves Corvo an exceptional massive sulfide deposit both in the IPB and worldwide (Relvas et al. 2001, 2006b; Tornos et al. 2005).

The Neves Corvo host succession is approximately 600 m thick (true thickness) and dominated by mudstone. The succession also includes three volcanic units, one of which is similar in age to, and spatially associated with, the ore bodies. In this paper, we describe and interpret the Neves Corvo host succession with emphasis on the volcanic lithofacies and provide constraints on the massive sulfide ore-forming environment and the timing of the mineralization with respect to volcanic events.

Geological setting

The massive sulfide deposits of the IPB are hosted by the Upper Devonian to Lower Carboniferous Volcanic-Sedimentary Complex (VSC), a bimodal predominantly felsic volcanic succession and dark gray and black mudstone (Oliveira 1990). The VSC typically varies from 100 to 600 m in true thickness, locally being 1,300 m thick (true thickness; Tornos 2006). This complex conformably overlies a shallow marine sedimentary unit, the Phyllite–Quartzite Group (Late Devonian, base unknown), and is overlain by thick turbidites of the Baixo Alentejo Flysch Group (Early to Late Carboniferous). Disruption of the IPB stratigraphy by low-angle thrust faults generated in a thin-skinned tectonic regime, and subsequent folding of the thrust sheets to form NW–SE and W–E trending anticlines, occurred during the Variscan orogeny in the Late Devonian-Carboniferous (Silva et al. 1990; Quesada 1998; Soriano and Casas 2002). Tectonic deformation involved concentration of strain in narrow zones (Silva et al. 1990) between which the succession remained relatively undisturbed so that primary textures and structures and contact relationships are commonly preserved.

The submarine depositional environment of the VSC is indicated by the widespread presence of diverse marine fossils (radiolaria, conodonts, dasycladales, and ammonoids) and abundant massive sulfide deposits throughout the belt. Much of the depositional setting of the VSC was below wave base as suggested by the common occurrence of thick (>400 m, true thickness) intervals of planar laminated or massive mudstone interbedded with volcaniclastic gravity current deposits. The water depth at the time of ore deposition at Neves Corvo is poorly constrained but was clearly below storm wave base as indicated by the occurrence of planktonic ammonoids (Korn 1997), the absence of traction current structures (Relvas 2000; this study), and the great thickness of dark gray and black mudstone in the footwall succession (Carvalho and Ferreira 1994; Oliveira et al. 2004).

The Neves Corvo Mine exploits one of the 85 massive sulfide deposits known in the IPB (Fig. 1; Leistel et al. 1998; Carvalho et al. 1999; Tornos 2006). It occurs at the southeastern termination of the NW–SE trending and southeast-plunging Rosário-Neves Corvo anticline in the Portuguese segment of the belt.

The five ore bodies (Corvo, Graça, Neves, Zambujal, and Lombador) at Neves Corvo are connected by thin massive sulfide lenses (ore bridges) which are conformable with the stratigraphy (Relvas et al. 2006a). Carvalho and Ferreira (1994), Oliveira et al. (2004) and Relvas et al. (2006a) reported that the massive sulfide ore bodies occur within a major thrust slice that was only locally tectonically disrupted. Apart from the massive sulfide lenses, this relatively undisturbed thrust slice also includes stockwork feeder zones, some of which are deeply rooted (e.g., Neves North-Lombador stockwork; Relvas 2000). Below the Corvo ore body, the sulfide stockwork extends for about 70 m down into the footwall (mudstone and the lower volcanic sequence) where it is truncated by a fault (Relvas 2000; Relvas et al. 2006a).

Methods and approach

This analysis of the volcanic and sedimentary host succession at Neves Corvo is based on the detailed logging and sampling of approximately 2,105 m of core from 17

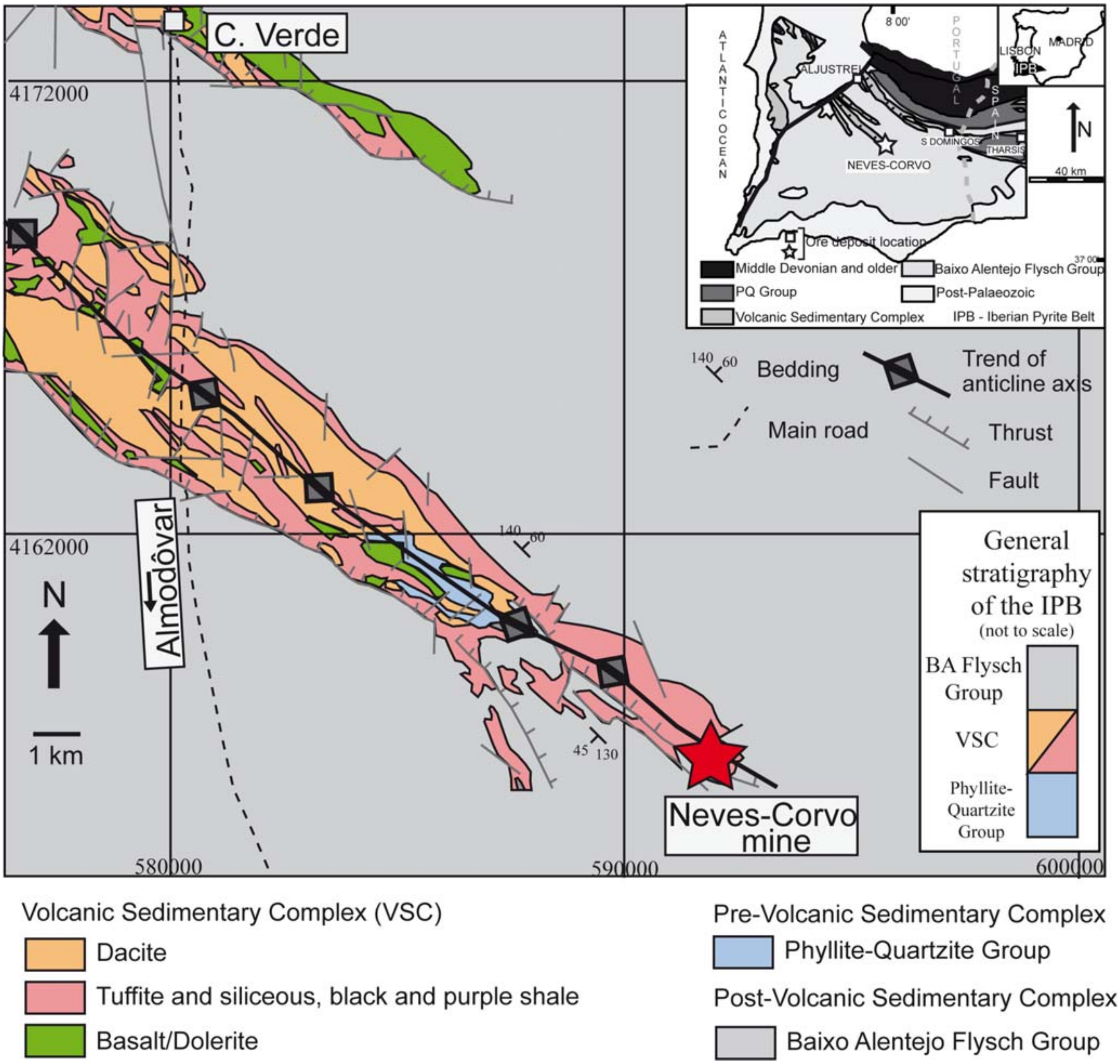

Fig. 1 Location of the Neves Corvo Mine in the Rosário-Neves Corvo antiform (adapted from Geological Map of Portugal, sheet 8, scale 1:200,000). *Inset map* shows location of the Iberian Pyrite Belt in the Iberian Peninsula and location of the Neves Corvo Mine in the Iberian Pyrite Belt, (adapted from Thiéblemont et al. 1998)

drill holes located within the mine lease (Fig. 2). The host succession is deeply buried, the nearest outcrops of volcanic rocks being about 3 km to the northwest of the mine area. Hence, no surface mapping was carried out.

The drill holes were made available for study by SOMINCOR, and most intersected the least-altered lithofacies in which original volcanic textures are well preserved apart from the strongly cleaved intervals close to faults. However, some of the drill holes intersected strongly altered and mineralized zones and were studied to identify possible relationships between hydrothermal activity and particular volcanic facies.

Textural and petrographic data were obtained on 150 samples taken from the 17 drill holes. A subset of 17 least altered samples, representing the major volcanic lithofacies identified, was analyzed for major and trace elements at Actlabs, Canada using the 4Litho research package. Details of the locations of the samples and of the analytical procedures including standards and duplicates are given in Rosa (2007).

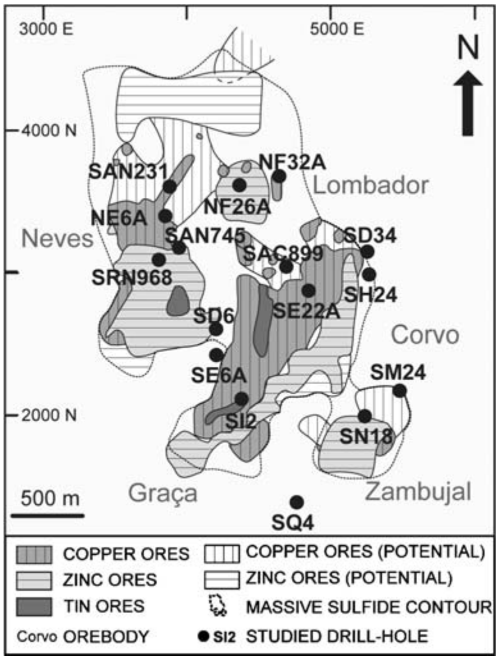

Fig. 2 Map of lateral zonation in metal content of the Neves Corvo Mine showing the location of the drill-holes used in this study and the Zambujal, Graca, Neves Corvo, and Lombador ore bodies (SOMINCOR 2000; unpublished document). Drill-hole MB1 is not shown on this map; it occurs approximately 2.5 km to the SE of the Zambujal orebody (coordinates, −545; 6765). Map grid from SOMINCOR

Stratigraphy and age of the Neves Corvo host succession

The biostratigraphy of the Neves Corvo Mine was recently defined by Oliveira et al. (2004) based on palynomorphs and ammonoid associations from about 700 samples collected in 39 drill holes. Their samples came from dark gray and black mudstone occurring close to the lower and upper contacts of both the massive sulfide ore bodies and the three major volcanic sequences in the host succession, informally referred to here as the lower, intermediate, and upper volcanic sequences. Most of the drill holes logged for this study were included in the palynological study of Oliveira et al. (2004) and Pereira et al. (2003), allowing the integration of the age data with the facies architecture. The lower and the intermediate volcanic sequences are relatively thick and laterally extensive over the mine area (Rosa et al. 2005). These two sequences occur stratigraphically beneath the massive sulfide ore bodies and are interleaved with relatively thin (up to 50 m) intervals of dark gray and black mudstone. The massive sulfide ore bodies directly overlie the intermediate volcanic sequence or mudstone (Rosa et al. 2005). A discontinuous layer of blue or gray chert and carbonate of hydrothermal origin overlie or are laterally equivalent to the massive sulfide ore bodies (Mirão et al. 1997; Relvas 2000). Above the massive sulfide ore bodies, there is a very thick succession (up to 400 m) of mudstone that includes the upper volcanic sequence. The upper volcanic sequence is less voluminous than the other two volcanic sequences (Rosa et al. 2005).

The host succession at Neves Corvo extends from the late Famennian (Upper Devonian) to the mid-late Visean (Lower Carboniferous). The lower volcanic sequence is late Famennian, and the intermediate volcanic sequence is late Strunian. The upper volcanic sequence is early Visean (Oliveira et al. 2004; Pereira et al. 2003). The late Strunian (Upper Devonian) age of the Neves Corvo massive sulfide ore bodies corresponds to the time span of 354.8 to 354.0 Ma (Oliveira et al. 2004). This age, based in biostratigraphic data, is consistent with the radiometric ages obtained for the Neves Corvo ores (Relvas et al. 2001; Munhá et al. 2005). Ages of the felsic volcanic rocks, from U/Pb isotopes in zircons, elsewhere in the IPB (Barrie et al. 2002) range from 356.2±0.73 Ma in Lagoa Salgada, Portugal to 349.7±0.9 Ma in Rio Tinto, Spain.

Oliveira et al. (2004) identified a stratigraphic hiatus of approximately one million years between the lower and the intermediate volcanic sequences. This hiatus corresponds to the early/middle Strunian. Two other stratigraphic hiatuses, above the stratigraphic level of the ore bodies, correspond to the entire Tournaisian and part of the early Visean.

Volcanic lithofacies

Fourteen lithofacies were identified in the Neves Corvo host succession, ten of which are volcanic. The remaining facies are fine-grained sedimentary facies (Table 1).

The three main volcanic sequences are each composed of a single volcanic facies association or facies that can be distinguished by composition and texture. Each volcanic sequence occurs in a distinct position in the stratigraphy and is intercalated with mudstone for most of their lateral extent (Fig. 3). The lower volcanic sequence consists of the rhyolitic fiamme-rich facies association (fiamme breccia facies, fiamme-crystal sandstone facies, and fiamme mudstone facies), the intermediate volcanic sequence consists of the rhyolite facies association (coherent rhyolite, jigsaw-fit, and clast-rotated monomictic rhyolite breccia, stratified monomictic rhyolite breccia, stratified crystal-rich sandstone, and sediment-rhyolite breccia), and the upper volcanic sequence consists of the dacitic jigsaw-fit breccia facies. A fourth distinctive but less voluminous lithofacies, the polymictic fiamme sandstone facies, occurs locally at the same stratigraphic level as the lower volcanic sequence and below the intermediate volcanic sequence.

Previous geochemical studies (Munhá et al. 1997) have shown that the volcanic rocks of Neves Corvo range from rhyolite to dacite but have not distinguished among the

Table 1 Summary of the principal volcanic and sedimentary facies of Neves Corvo

Lithofacies	Characteristics	Interpretation
Rhyolitic fiamme-rich facies association		
Fiamme breccia	Massive, thick, poorly sorted and coarse. Components: quartz-phyric fiamme (quartz is euhedral to sub-euhedral and up to 2 mm across), quartz crystal fragments, dense felsic clasts, black mudstone and chert. In places is silicified, altered to chlorite and sericite and has abundant disseminated sulfides. Thickness: up to 45 m	Eruption-fed pyroclastic deposit. Deposition from high-density gravity currents
Fiamme-crystal sandstone	Thick and massive or normally graded. Clast-supported. Compositionally similar, but finer grained than the fiamme breccia. Additionally contains abundant quartz crystals and crystal fragments. Thickness: up to 15 m	Eruption-fed pyroclastic deposit. Deposition down-current from the high-density gravity currents that sourced the fiamme breccia
Fiamme mudstone	Massive, or diffusely laminated, containing abundant cuspate and angular phyllosilicates in the matrix (glass shards?). Contains outsize fiamme. In places is silicified, altered to chlorite and sericite and has abundant disseminated sulfides. Thickness, ~7 m	Eruption-fed pyroclastic deposit. Deposition from the dilute parts of the high-density gravity currents, and by water settling
Polymictic fiamme sandstone facies		
Polymictic fiamme sandstone facies	Thinly or thickly bedded. Moderately sorted, massive or normally graded. Components: Abundant quartz and feldspar crystal fragments, felsic clasts, black mudstone and limestone clasts, and rare fiamme. Locally is silicified, and altered to chlorite and sericite or with abundant disseminated sulfides. Thickness, >60 m	Distal pyroclastic deposit, or remobilisation of previously deposited non-consolidated volcanic debris. Deposition from low-density gravity currents
Rhyolite facies association		
Coherent rhyolite	Evenly quartz- and feldspar-phyric (10–20 vol.%); rare biotite phenocrysts. Groundmass micropoikilitic, spherulitic and locally perlitic with amygdales (up to 7%, 1 mm to 2 cm, filled with quartz, carbonates and chlorite). Rare flow bands (0.5–1 cm thick). Flow bands are spherulite- and phyllosilicate-rich, or quartz-feldspar. Thickness, 3–10 m	Coherent facies of lavas or domes
Jigsaw-fit and clast-rotated monomictic rhyolite breccia	Monomictic, poorly sorted, and typically clast-supported. Jigsaw-fit rhyolite clasts that have groundmass textures similar to the coherent facies, but are more perlitic. The clasts are slabby, irregular and blocky, 1–50 cm across, with planar and curviplanar margins. The matrix consists of fine rhyolite clasts, crystals and crystal fragments (<2 mm). Thickness, 40–250 m. The clast rotated intervals are similar to the jigsaw-fit breccia, but have more matrix and show abundant clast-rotated textures. Thickness, 1–120 m	In situ and clast-rotated hyaloclastite and autobreccia
Stratified monomictic rhyolite breccia	Monomictic, massive or normally graded, poorly sorted, clast- to matrix-supported. The clasts are similar to clasts in the jigsaw-fit and clast-rotated monomictic rhyolite breccia. Thickness, 12 m	Redeposited hyaloclastite and autobreccia
Stratified crystal-rich sandstone	Relatively well sorted, thinly bedded, massive, or normally graded. Components: quartz and feldspar crystal fragments, fine rhyolite clasts and rare chert and carbonate clasts Thickness, up to 10 m	Redeposited fine volcanic debris
Sediment-rhyolite breccia	Poorly sorted, non-stratified, clast- to matrix-supported. Components: blocky rhyolite clasts, feldspar and quartz crystal fragments. Matrix: black mudstone. The black mudstone is massive or shows contorted	Peperite

Table 1 (continued)

Lithofacies	Characteristics	Interpretation
	lamination. This facies is restricted to the lower contact of the rhyolite facies association. Thickness, 1 m	
Dacitic jigsaw-fit breccia facies		
Dacitic jigsaw-fit breccia facies	Monomictic, massive, poorly sorted, clast- to matrix-supported. Abundant jigsaw-fit and clast-rotated textures. The dacite is quartz- and feldspar-phyric, or feldspar glomeroporphyritic. Clasts are blocky and angular with planar and curviplanar margins. Sharp contact with the overlying mudstone facies. Irregular and discordant contact with the underlying mudstone facies. Thickness, 30 m	*In situ* and clast-rotated hyaloclastite of lava or sill
Chert and carbonate facies association		
Chert	Massive, light gray beds. The beds are thin (10–20 cm), often disrupted and laterally discontinuous. Part of the "JC-jasper and carbonate unit" unit (mine nomenclature). Thickness, ~70 cm	Hydrothermal origin
Carbonate	Massive and brown. Occurs associated with the chert. Part of the "JC-jasper and carbonate unit" unit (mine nomenclature). Thickness, ~30 cm	Hydrothermal origin
Mudstone facies		
Mudstone	Massive, or thinly bedded. The mudstone is siliceous, chloritic and sericitic, and green, gray, or black. The black mudstone is rich in organic matter. Thickness: up to 200 m	Water settling of hemipelagic mud and/or volcanic ash
Limestone facies		
Limestone facies	Calcitic or dolomictic in massive thin beds. The limestone beds are disrupted and form boudins near foliated intervals. Thickness: up to 5 cm	Carbonate sedimentation with biogenic or chemical origin

different volcanic sequences. Our geochemical data (Rosa 2007) show differences between the lower (rhyolitic fiamme-rich facies association) and the intermediate (rhyolite facies association) volcanic sequences, although on classification diagrams, both associations are rhyolitic. These data also indicate that the dacitic jigsaw-fit breccia facies is dacitic.

Rhyolitic fiamme-rich facies association

The rhyolitic fiamme-rich facies association is characterized by the presence of abundant quartz-phyric fiamme (Fig. 4a and b). The groundmass of the fiamme is composed of fine-grained phyllosilicates and minor quartz and feldspar. No vesicular texture is preserved in the groundmass, and the fiamme are lenticular and aligned parallel to bedding. Equant, angular lithic clasts are also present.

The fiamme are considered to have originally been pumice clasts because: (1) their porphyritic texture indicates an igneous origin, (2) their elongate shape and bedding-parallel alignment contrasts with the equant shape of adjacent lithic clasts, indicating that the fiamme have been compacted, and hence, were probably originally vesicular, and (3) very coarse fiamme occur in laminated mudstone (fiamme mudstone facies), suggesting that the coarse fiamme and much finer mud were simultaneously deposited from suspension and therefore had similar low settling velocities. The high abundance (>70 modal %), relatively fine grain size (most are <2 mm across) and the ragged margins of the fiamme suggest a pyroclastic origin for the original pumice clasts. Flattening of the pumice clasts probably occurred when vesicles were empty, and the glassy vesicle walls were altered so the clasts do not preserve any internal vesicular texture (e.g., McPhie and Allen 2003; Gifkins et al. 2002).

The rhyolitic fiamme-rich facies association is interbedded with dark gray and black mudstone. The fiamme breccia, fiamme-crystal sandstone, and fiamme mudstone facies define two polymictic and overall graded fiamme breccia units (subunit A and subunit B). Subunit A is typically very thick (up to 60 m) and has an irregular, discordant, and erosional basal contact with black mudstone. Subunit B is thinner (up to 20 m) and more intensely hydrothermally altered than subunit A. Subunit B overlies subunit A at an irregular and erosional or faulted contact (Fig. 5). The two graded subunits occur in the southern part of the Neves Corvo Mine and have similar internal structure and compositions.

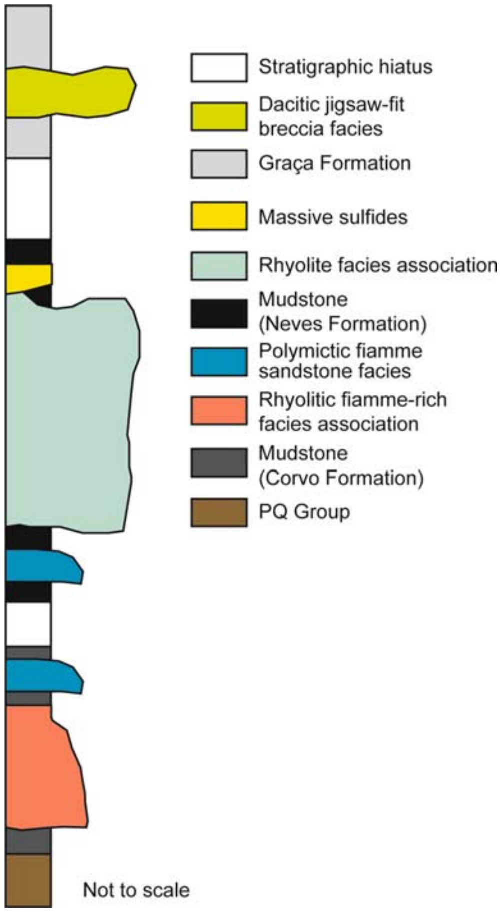

Fig. 3 Simplified stratigraphic column for the Neves Corvo Mine (not to scale)

The lower part of both subunits consists of fiamme breccia facies. This part is thick (45 m on average for subunit A and 10 m for subunit B), massive, poorly sorted, and polymictic, being composed of fiamme (Fig. 6a), irregular and angular clasts of black mudstone (Fig. 6b), dense spherulitic rhyolite clasts, and quartz crystal fragments. The intermediate part consists of fiamme-crystal sandstone facies. This part is thinner (15 m thick on average for subunit A and 5 m for subunit B), massive (Fig. 6c) and finer grained than the lower part, and dominantly composed of fiamme and quartz crystal fragments. The top part (7 m thick on average for subunit A and 5 m for subunit B) consists of fiamme mudstone facies and comprises massive or diffusely laminated siliceous mudstone that contains fiamme up to 6–10 cm across (Fig. 6d). Contacts between adjacent facies are gradational, as are contacts with the overlying sedimentary facies. Subunit B lacks black mudstone clasts in the lower part, containing instead abundant gray siliceous mudstone clasts similar to the mudstone that forms the top part of subunit A.

The two graded subunits are interpreted to consist mainly of juvenile pyroclasts (fiamme that were formerly pumice and quartz crystal fragments). The minor lithic clasts include both vent-derived (felsic volcanic clasts) and accidental (mudstone clasts and volcanic clasts?), non-juvenile clasts. Despite being largely composed by juvenile pyroclasts and occurring in very thick beds, the fiamme breccia subunits show no evidence for hot emplacement. Therefore, the compaction of pumice to form fiamme was more likely to have been diagenetic than a result of hot welding compaction. The internal organization of each subunit is typical of deposits from high-concentration, voluminous water-supported gravity currents (Lowe 1982), which, given the great thickness of the beds and dominance of juvenile pyroclasts, were fed directly by explosive eruptions. The locations of the source vents for the explosive eruptions are uncertain. Nevertheless, the high abundance of pumiceous (now fiamme) ash and lapilli, the absence of subaerially derived lithic clasts, and the relatively good hydraulic sorting are consistent with the source vents being submarine (e.g., McPhie and Allen 2003; Kano et al. 1996). In addition, both subunits A and B are restricted to the southern part of the Neves Corvo Mine and show lateral variations consistent with a local, hence intrabasinal, source vent location.

Towards the north and south of the mine lease, subunits A and B are represented by two fiamme-crystal sandstone-rich subunits. In addition, the intervals of

Fig. 4 **a** Photomicrograph (transmitted light, crossed nicols) of phyllosilicate-rich fiamma (*FL*) with quartz phenocrysts (SI2, 315.50 m). **b** Photomicrograph (transmitted light, crossed nicols) of a phyllosilicate lense (fiamma) showing a quartz phenocryst broken at the edge of the fiamma (*arrow*) (SN18, 533.50 m)

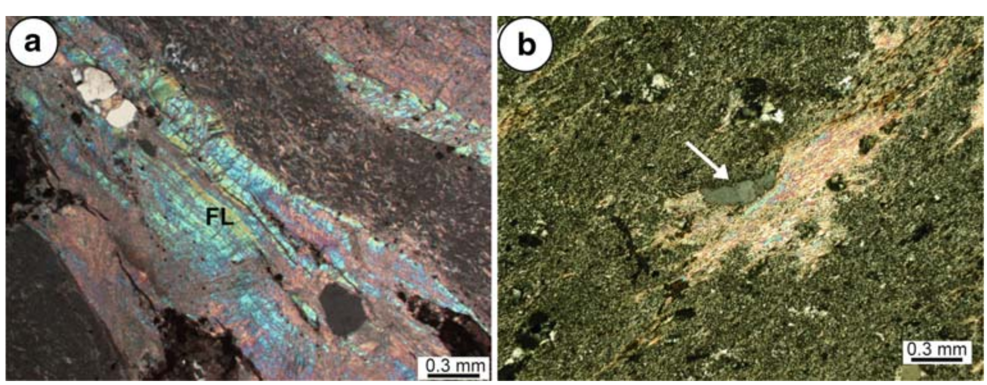

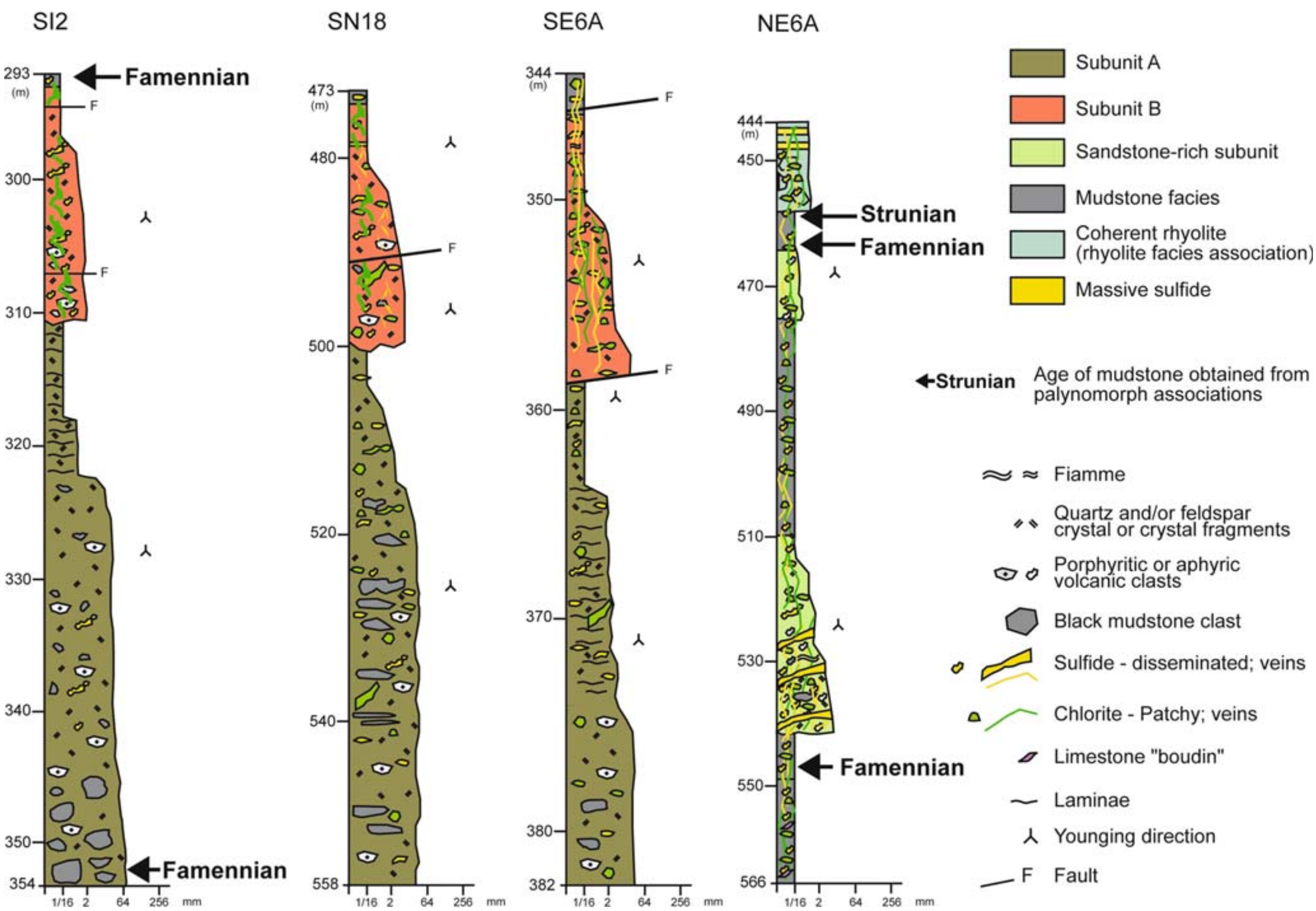

Fig. 5 Logs of representative drill-holes that have intersected the rhyolitic fiamme-rich facies association showing the graded subunits A and B and the fiamme-crystal sandstone-rich subunits. See Fig. 2 for location of the drill-holes. Logs are at different scales

fiamme breccia facies in each subunit become progressively less common and thinner, whereas the fiamme-crystal sandstone and fiamme mudstone facies become abundant and relatively thick (Fig. 7). This trend is taken to indicate that the main area where subunits A and B are thick and coarse was the most proximal to source. In the distal zones, the fiamme breccia facies and fiamme-crystal sandstone facies occur in tabular beds, are relatively well-sorted, and contain relatively abundant outsize fiamme (Fig. 6e). Alternatively, this decrease in thickness and grain size of the fiamme-rich facies, away from the southern area of the Neves Corvo Mine, could relate to palaeotopography, the thicker and coarser intervals occurring within a palaeotopographic low (fault controlled?) and the thinner and finer grained facies being on marginal highs.

Polymictic fiamme sandstone facies

Intervals of the polymictic fiamme sandstone facies are up to 10 m thick and occur only in the central part of the Neves Corvo area, intercalated with mudstone. The mudstone yielded palynomorphs assigned to late Famennian or Strunian age (Fig. 8). Therefore, units of this facies are coeval with and younger than the lower volcanic sequence (rhyolitic fiamme-rich facies association) and underlie the intermediate volcanic sequence (rhyolite facies association). Single beds are either massive (Fig. 8a), or normally graded, well sorted, and up to 1 m thick. The polymictic fiamme sandstone facies comprises feldspar and quartz crystal fragments, black mudstone clasts, felsic volcanic clasts, quartz-phyric phyllosilicate fiamme (former pumice clasts), and limestone clasts (Fig. 8b).

This facies resembles the fiamme-crystal sandstone facies of the rhyolitic fiamme-rich facies association but is much less voluminous, better sorted, more distinctly bedded, and contains fewer fiamme. The abundant fine-grained volcanic components (quartz and feldspar crystal fragments, felsic clasts, and fiamme) were probably sourced from explosive eruption(s) of felsic magma. The diffuse and normally graded nature of the beds indicates deposition from moderate- to high-concentration gravity currents. These currents incorporated abundant intrabasinal clasts (mudstone and limestone) during transport.

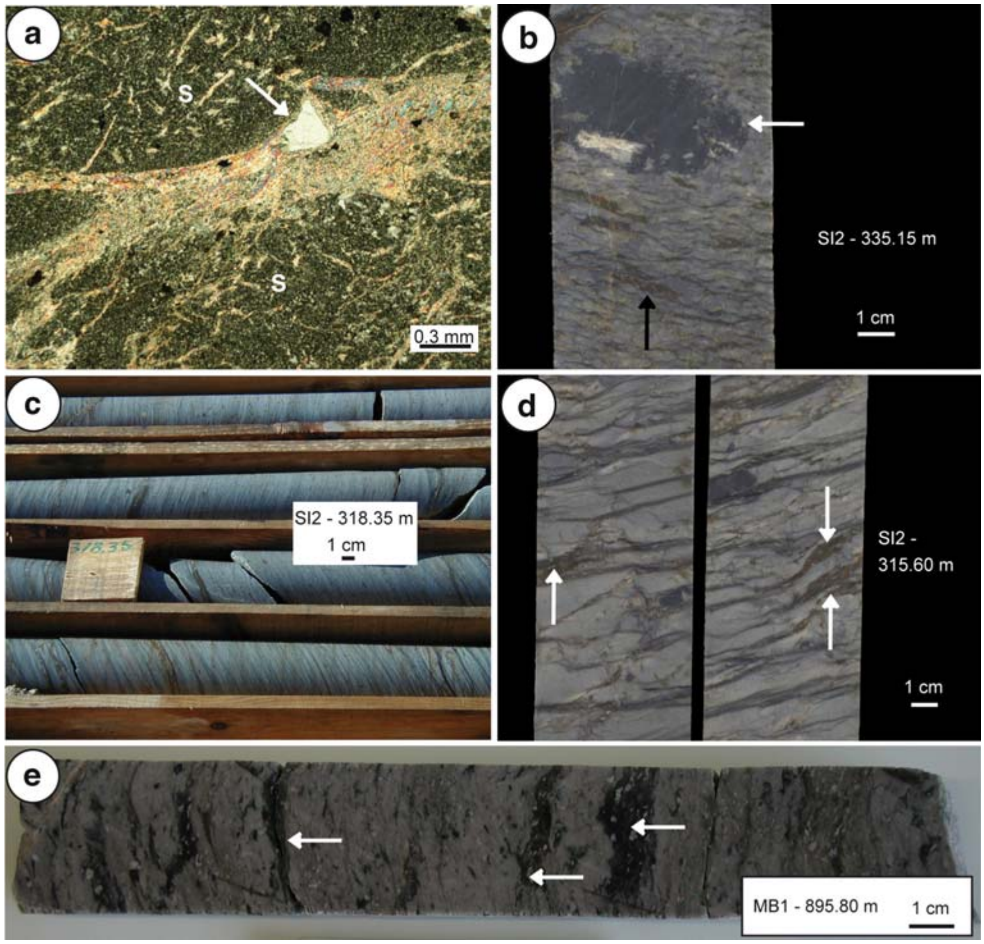

Fig. 6 Rhyolitic fiamme-rich facies association. **a** Photomicrograph (transmitted light, crossed nicols) of a fiamma with a quartz phenocryst broken at the edge of the clast (*arrow*; SI2, 313.60 m); platy and cuspate phyllosilicate shapes in the matrix may be altered glass shards (*S*). **b** fiamme breccia facies showing a mudstone clast with irregular margins (*white arrow*) and fiamme (*black arrow*; SI2, 335.15 m). **c** fiamme-crystal sandstone facies (SI2, 318.35 m). **d** fiamme mudstone facies showing abundant outsize fiamme (*arrows*; SI2, 315.60 m). **e** fiamme-crystal sandstone showing coarse (>3 cm) fiamme (*arrows*; MB1, 895.80 m)

Rhyolite facies association

The rhyolite facies association extends throughout the entire Neves Corvo area, except for the westernmost part, and constitutes the intermediate volcanic sequence stratigraphically above the rhyolitic fiamme-rich facies association. The rhyolite facies association is interbedded with dark gray and black mudstone that contains palynomorph assemblages typical of the Western European LN biozone, which is late Strunian in age (Fig. 9; Oliveira et al. 2004).

This facies association comprises intervals of coherent quartz–feldspar–phyric rhyolite that are compositionally and texturally uniform throughout the Neves Corvo area. These intervals are up to 10 m thick and enclosed by much thicker intervals (85 to 135 m thick, but up to 250 m) of jigsaw-fit and clast-rotated monomictic rhyolite breccia (Fig. 9). Typical groundmass textures include microcrystalline quartz–feldspar–phyllosilicate assemblages, rare amygdales filled by quartz and calcite and narrow (0.1–2 cm thick) flow bands (Fig. 10a). The flow bands are defined by alternating quartz–feldspar microcrystalline groundmass and phyllosilicate-rich bands that contain abundant and well-preserved spherulites (Fig. 10b).

The contacts between the jigsaw-fit and clast-rotated monomictic rhyolite breccia facies and the coherent rhyolite facies are gradational. The groundmass textures and phenocryst assemblages of the clasts in the breccias are identical to those of the coherent rhyolite. However, clast groundmasses are dominated by phyllosilicates, display abundant perlitic cracks (Fig. 10c), and contain only rare spherulites. The jigsaw-fit and clast-rotated monomictic rhyolite breccia domains are non-stratified, monomictic, and poorly sorted. Most are clast-supported, although matrix-supported intervals also occur. The clasts occur in a matrix of compositionally similar, finer rhyolite clasts and crystal fragments. The clast margins are planar or curviplanar, and clast shapes are blocky, irregular, or tabular (Fig. 10d). Margins of tabular flow-banded clasts are generally parallel to flow bands. The jigsaw-fit monomictic rhyolite breccia typically shows jigsaw-fit organization of the clasts (Fig. 10e).

The clast shapes, the jigsaw-fit and dominant perlitic texture, and the monomictic composition of the jigsaw-fit and clast-rotated monomictic rhyolite breccias are typical of hyaloclastite (e.g., Pichler 1965; Yamagishi 1987). Domains of the breccia where clasts are blocky and flow

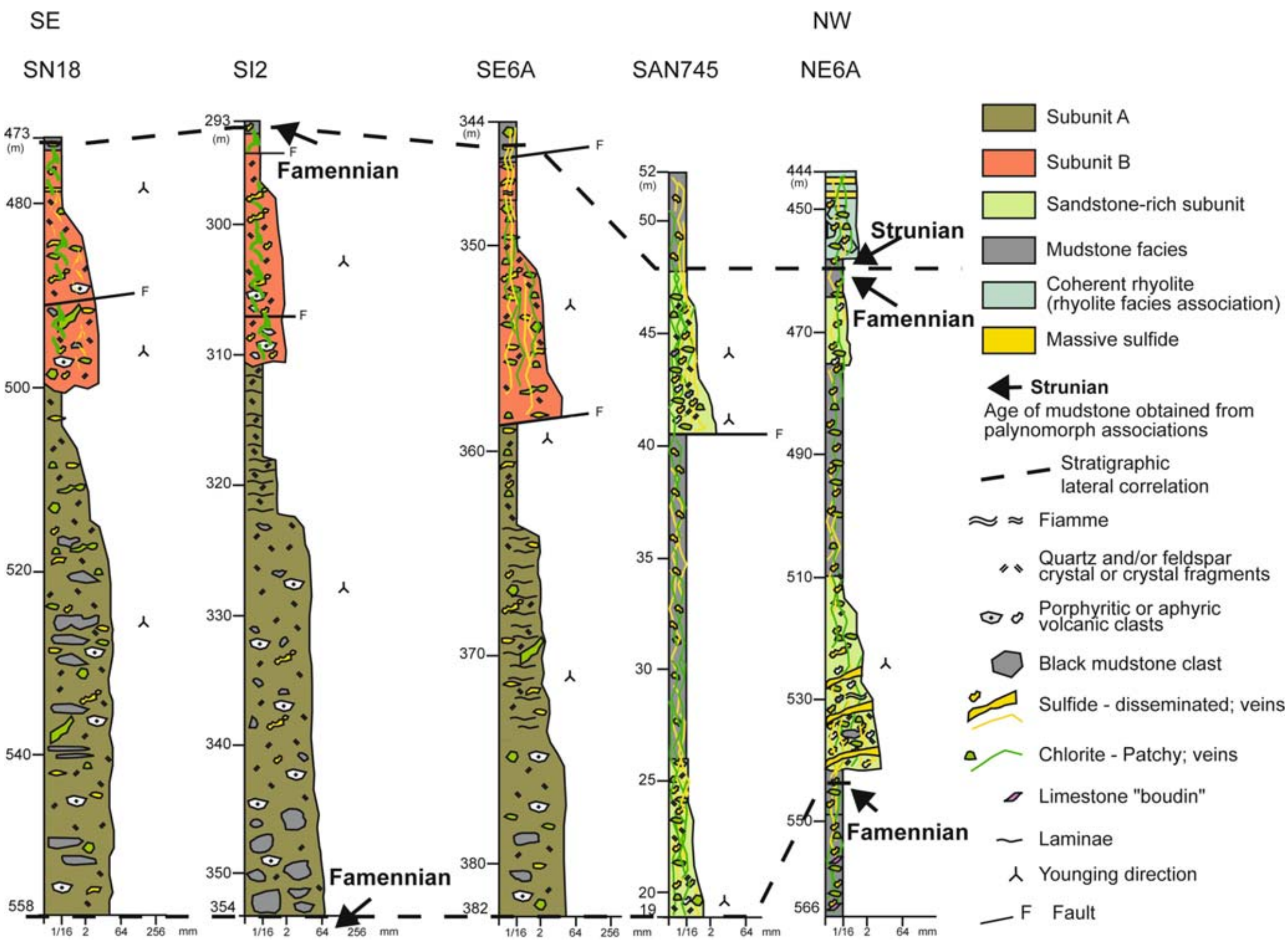

Fig. 7 Stratigraphic lateral correlation of units of the rhyolitic fiamme-rich facies association across the Neves Corvo Mine. See Fig. 2 for location of the drill-holes. Logs are at different scales

banded may be autobreccia; however, hyaloclastite is largely dominant. The angularity of the clasts and presence of jigsaw-fit texture in the jigsaw-fit monomictic rhyolite breccia indicate that fragmentation occurred in situ (in situ hyaloclastite and autobreccia).

Beds of stratified monomictic rhyolite breccia alternating with beds of stratified crystal-rich sandstone either gradationally overlie or occur laterally adjacent to the jigsaw-fit and clast-rotated monomictic rhyolite breccia domains. These facies occur in intervals up to 10 m thick in which bedding is poorly defined (Fig. 10f). The stratified monomictic rhyolite breccia and crystal-rich sandstone facies are interpreted as the products of down-slope redeposition of unconsolidated hyaloclastite, as they comprise clasts similar in composition and texture to those in the jigsaw-fit and clast-rotated monomictic rhyolite breccias. The stratified monomictic rhyolite breccia and crystal-rich sandstone facies grade into overlying gray, black, or green siliceous mudstone.

The rhyolite facies association also includes the sediment-matrix rhyolite breccia facies which typically occurs at the base of the association. This facies is thin (up to 1 m thick), massive and unsorted, and has gradational contacts with the overlying jigsaw-fit and clast-rotated monomictic rhyolite breccia and also with the underlying mudstone. The sediment-matrix rhyolite breccia comprises irregular rhyolite clasts and crystal fragments scattered in a mudstone matrix that is either massive or has locally disturbed lamination. The characteristics of the sediment-matrix rhyolite breccia are consistent with blocky peperite (Kokelaar 1986) generated by local mingling of coherent rhyolite and hyaloclastite with unconsolidated mud.

The gradational contacts between all facies of the rhyolite facies association coupled with their uniform composition indicate they are genetically related. This association comprises coherent rhyolite, rhyolitic hyaloclastite and minor autobreccia, and has an internal architecture typical of submarine silicic lavas (e.g., McPhie et al. 1993). The extrusive setting of the association is indicated by the gradational transition of the hyaloclastite (jigsaw-fit and clast-rotated monomictic rhyolite breccia) to the overlying sedimentary facies and the relatively abundant beds of redeposited hyaloclastite (stratified monomic-

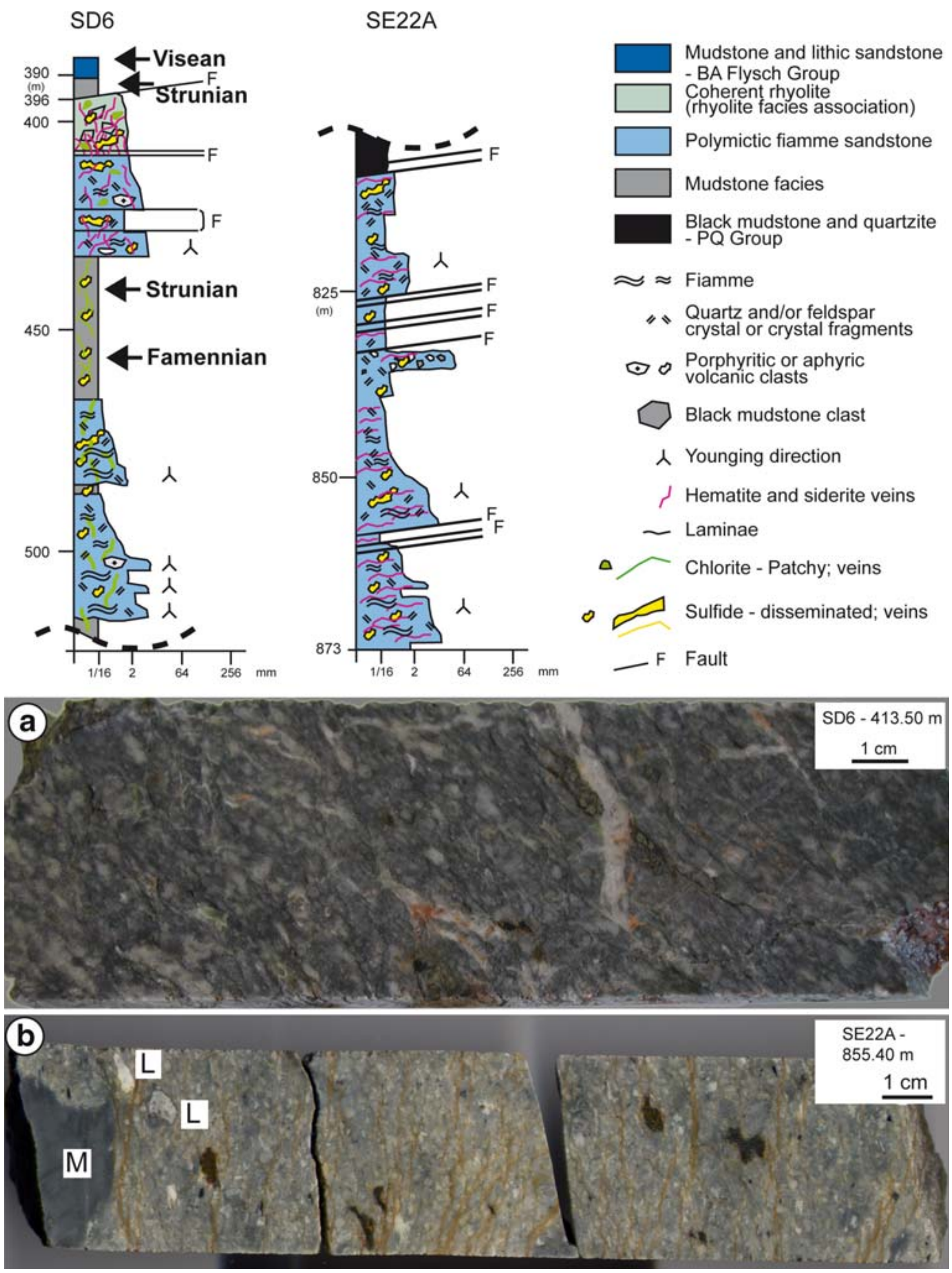

Fig. 8 Partial logs of the polymictic fiamme sandstone facies. **a** Massive single bed of polymictic fiamme sandstone consisting of quartz, feldspar and fiamme crystal fragments (SD6, 413.50 m). **b** Single bed of polymictic fiamme sandstone consisting of quartz, feldspar and fiamme crystal fragments, felsic volcanic clasts (*L*), and a mudstone clast (*M*; SE22A, 855.40 m). See Fig. 2 for location of the drill-holes. Logs are at different scales

tic rhyolite breccia and crystal-rich sandstone facies). The lava consisted of a relatively thin (3–10 m) coherent core surrounded by thick (up to 250 m) intervals of in situ hyaloclastite with tops and marginal aprons of redeposited hyaloclastite (Fig. 9). The peperite at the base indicates that the rhyolitic lava flowed over unconsolidated and probably wet mud.

The studied drill-holes are too widely separated to positively determine if all the intersected intervals of this facies association are parts of the same lava, or parts of different lavas, or parts of a complex of domes. Nevertheless, all single intersections of the rhyolite facies association have similar thickness and similar composition and groundmass textures, which suggest that the rhyolite facies association may well represent a single lava. Multiple intersections of the rhyolite facies association in drill core are typically separated by faults, suggesting that tectonic repetitions may have occurred. The exception is the top part of drill-hole NF32A (see Fig. 9 and Fig. 2) that shows a mudstone interval (approximately 5 m thick) between two intervals of the rhyolite facies association, suggesting they may correspond to two different lavas. The top part of both intervals

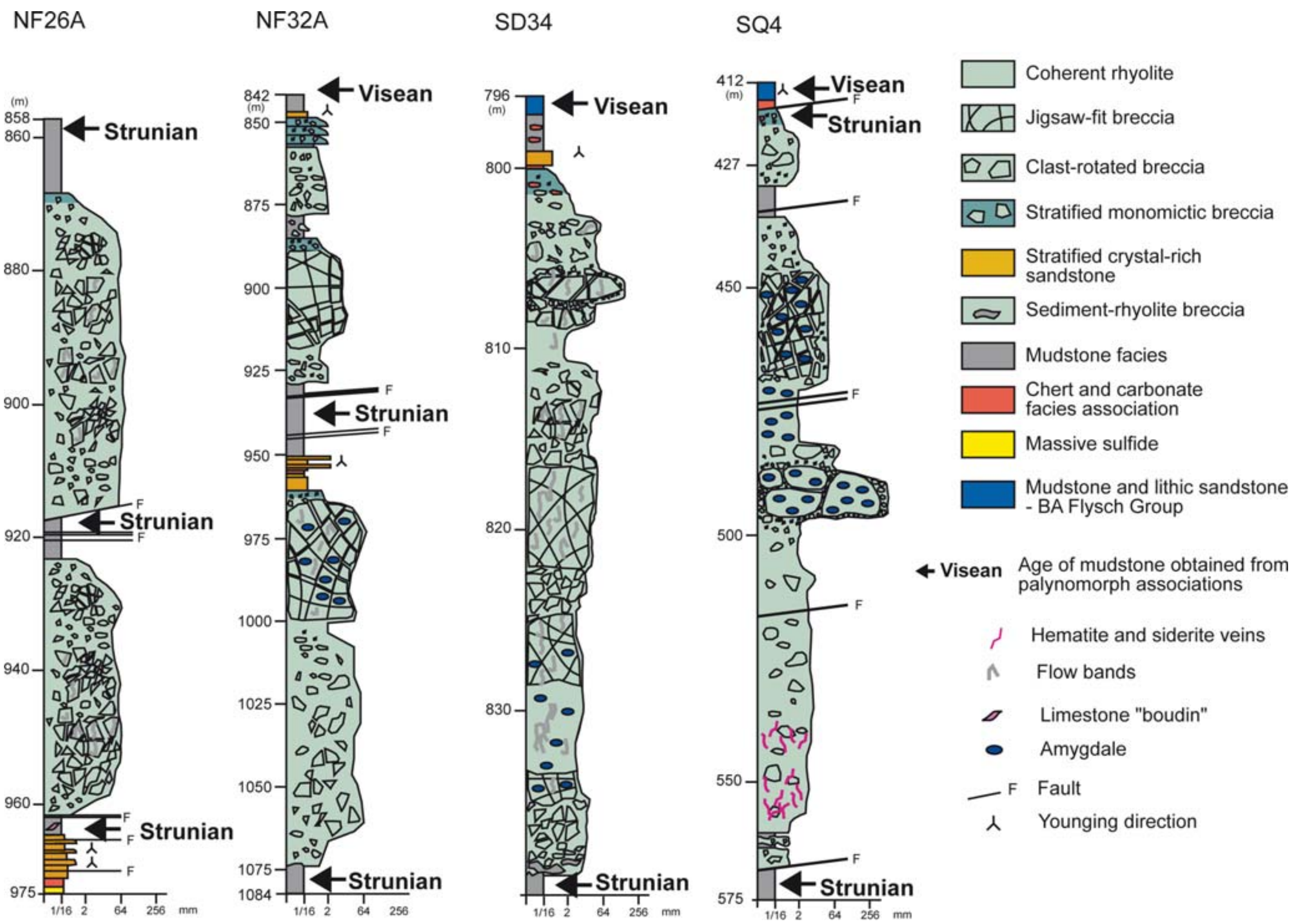

Fig. 9 Logs of representative drill-holes that have intersected the rhyolite facies association. See Fig. 2 for location of the drill-holes. Logs are at different scales

comprises beds of stratified monomictic rhyolite breccia alternating with beds of stratified crystal-rich sandstone, which suggest that both intervals of the rhyolite were extrusive.

Dacitic jigsaw-fit breccia facies

This facies forms the upper volcanic sequence and is intercalated with siliceous mudstone stratigraphically above the rhyolite facies association. It was intersected only in drill-hole MB1 approximately 2.5 km southeast of the Zambujal ore body (Fig. 11). The interval of dacitic jigsaw-fit breccia facies is 20 m thick and consists of monomictic, clast-supported jigsaw-fit breccia composed of feldspar-phyric dacite clasts. The clasts have planar and curviplanar margins and abundant perlitic fractures in the groundmass, which are consistent with brittle fragmentation of glassy clasts (Pichler 1965), probably as a result of quenching. The top contact of the dacitic jigsaw-fit breccia facies with siliceous mudstone is sharp. However, the absence of definitive information on the nature of the top contact of the dacitic jigsaw-fit breccia facies precludes determining the mode of emplacement.

Sedimentary lithofacies

The sedimentary facies at Neves Corvo comprise massive to thinly bedded mudstone units in which volcanic particles are absent or minor in abundance (Table 1). Using palynological data, Oliveira et al. (2004) and Pereira et al. (2003) recognized seven separate formations named from oldest to youngest Corvo, Neves, Graça, Grandaços, “Borra de Vinho”, Godinho, and Brancanes Formations. The Corvo Formation occurs at the base of the VSC and encloses the lower volcanic sequence (rhyolitic fiamme-rich facies association) and part of the polymictic fiamme sandstone facies. The Neves Formation encloses part of the polymictic fiamme sandstone facies, the intermediate volcanic sequence (rhyolite facies association), and the massive sulfide ore bodies. The Graça Formation probably

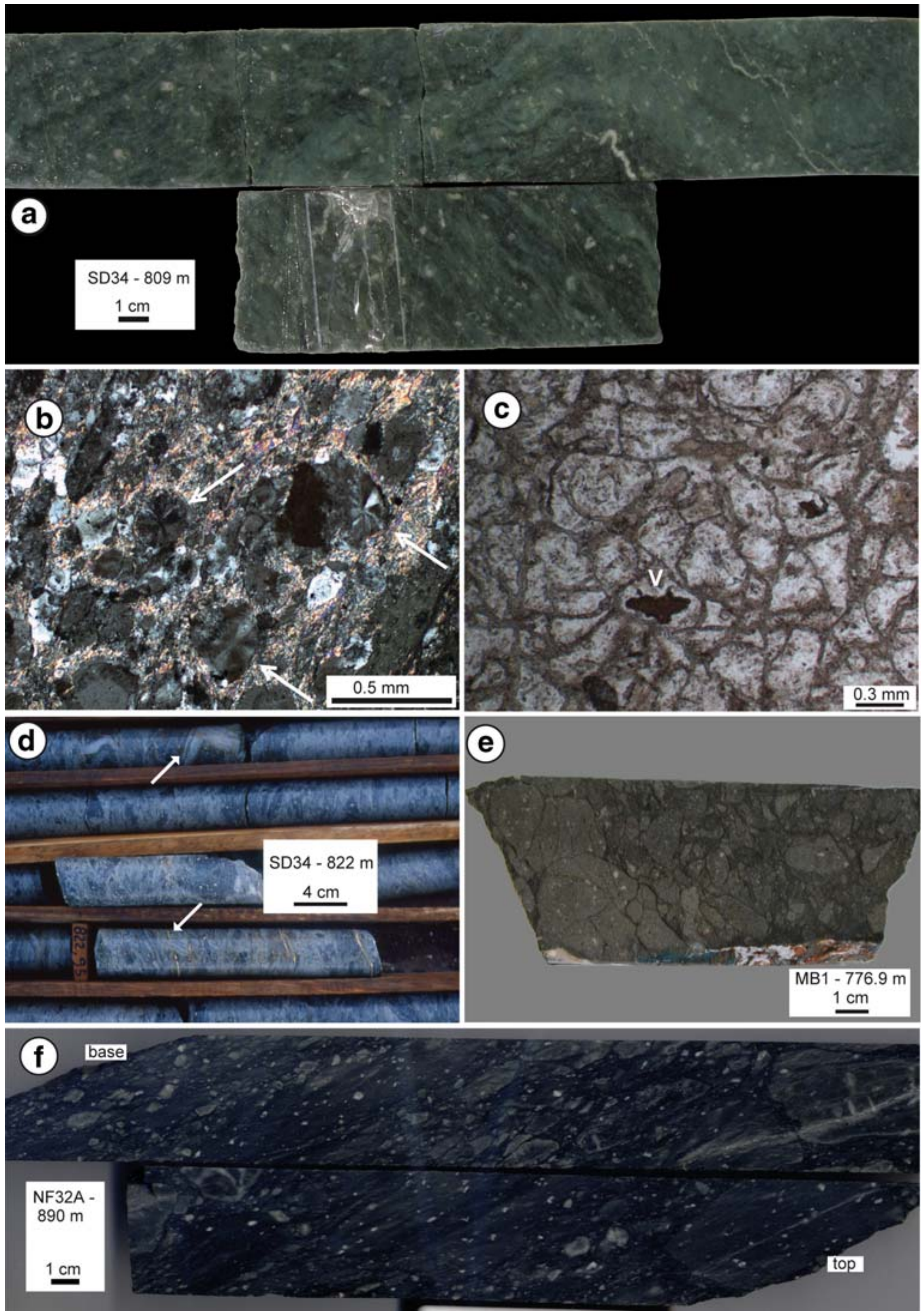

Fig. 10 Rhyolite facies association. **a** Detail of the flow banded rhyolite (SD34, 809.00 m). **b** Photomicrograph (transmitted light, crossed nicols) of spherulites (*arrows*) in a phyllosilicate-rich groundmass (NF32A, 851.05 m). **c** Photomicrograph (transmitted light, plane-polarized light) of perlitic cracks (NF32A, 971.70 m); *V* chlorite-filled amygdale. **d** Flow-banded clasts with random orientations (*arrows*) in the clast-rotated breccia (SD34, 822.00 m); *top to the right*. **e** Jigsaw-fit texture (*left*) grading to clast-rotated texture (*right*; MB1, 776.90 m). **f** Stratified poorly sorted breccia (NF32A, 890.00 m)

encloses the upper volcanic sequence (dacitic jigsaw-fit breccia facies). The Grandaços, “Borra de Vinho”, Godinho, and Brancanes Formations collectively account for up to 440 m of the total thickness of the VSC at Neves Corvo. These formations overlie the volcanic sequences and the massive sulfide ore bodies and extend in age up to the mid-late Visean.

Planar bedded, laterally continuous limestone units (calcitic or dolomitic) are locally intercalated with the mudstone facies and typically disrupted into “boudins” in proximity to strongly deformed, foliated intervals.

Relationship between volcanic sequences, ore, and altered zones at Neves Corvo

The hydrothermal activity that generated the massive sulfide ore bodies at Neves Corvo also altered all the

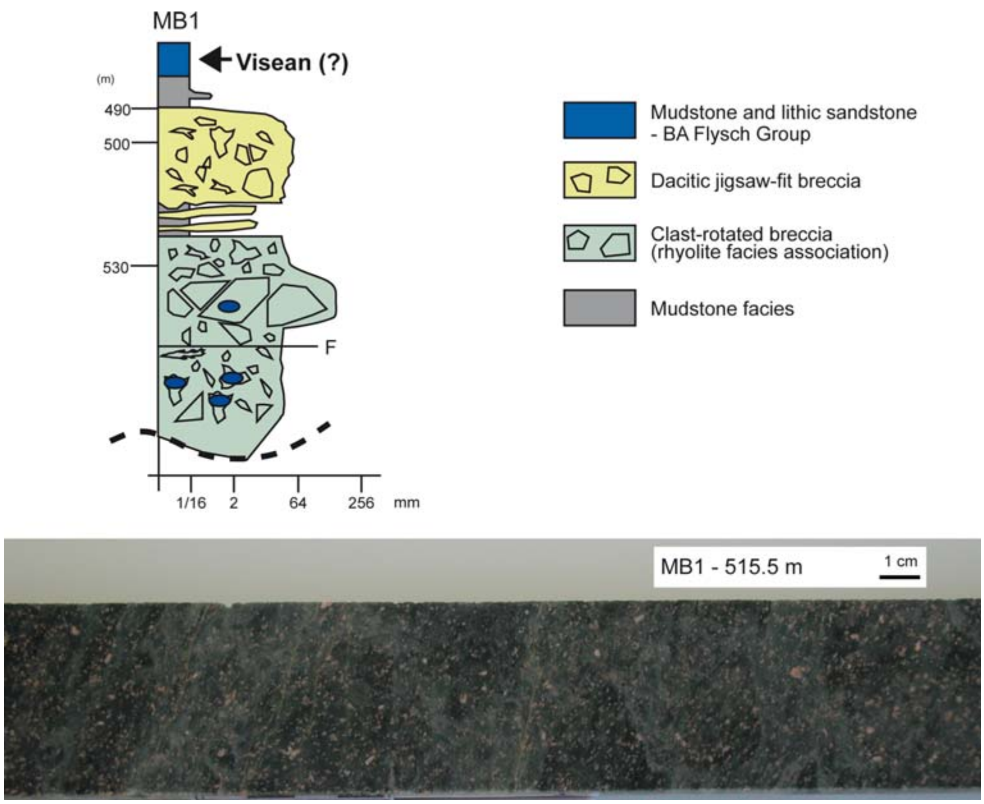

Fig. 11 Dacitic jigsaw-fit breccia facies in drill-hole MB1 showing its relation to the mudstone facies. Photograph shows the dacitic breccia (MB1, 515.50 m). Drill-hole MB1 is located approximately 2.5 km to the SE of the Zambujal orebody (see Fig. 2)

footwall volcanic facies, with variable intensity, regardless of the facies type. The morphology of the stockworks and disseminated ore clearly correlates with differences in the facies type, which could reflect the influence of original porosity and permeability on interaction with the mineralizing hydrothermal system. The lower volcanic sequence typically hosts disseminated, widespread, and stratabound stockworks (Relvas 2000; Rosa et al. 2005; Relvas et al. 2006a), consistent with the very high porosity and permeability expected for clastic pumiceous facies (rhyolitic fiamme-rich facies association). In contrast, the intermediate volcanic sequence typically hosts vein-dominated and cone-shaped stockworks in which veins have sharp contacts, reflecting the fracture-controlled porosity and permeability of coherent and jigsaw-fit breccia (rhyolite facies association; Relvas 2000; Rosa et al. 2005; Relvas et al. 2006a). Widespread replacement textures of the host lithologies by the sulfide ores have been identified (Relvas 2000; Rosa et al. 2005; Relvas et al. 2006a), particularly at the transition from the stockworks to the massive sulfide ore.

Oliveira et al. (2004) showed that both the ore bodies and their immediate host rocks (intermediate volcanic sequence–rhyolite facies association) are enclosed by dark gray and black mudstone of late Strunian age. The lower volcanic sequence (rhyolitic fiamme-rich facies association) is approximately one million years older than this (late Famennian) and, thus, is unlikely to be genetically related to the mineralization. This age difference also indicates that the lower and intermediate volcanic sequences were the products of separate volcanic eruptions and probably separate volcanic centres, although their phenocryst populations and magma compositions are similar.

Facies architecture evolution of Neves Corvo

Three main volcanic events, now very well constrained in time, generated the volcanic succession at Neves Corvo. Volcanism followed a long period of submarine sedimentation, recorded by thick dark gray to black mudstone interbedded with siliciclastic mudstone and sandstone, especially towards the top (Phyllite–Quartzite Group; Upper Devonian and older, base unknown). In the Neves Corvo area, the oldest sedimentary unit of the VSC is the Corvo Formation, a late Famennian mudstone unit variably rich in organic matter.

Late Famennian volcanism

The first volcanic activity at Neves Corvo occurred in the late Famennian and is represented by the lower volcanic sequence (rhyolitic fiamme-rich facies association). This activity was explosive and generated two successive

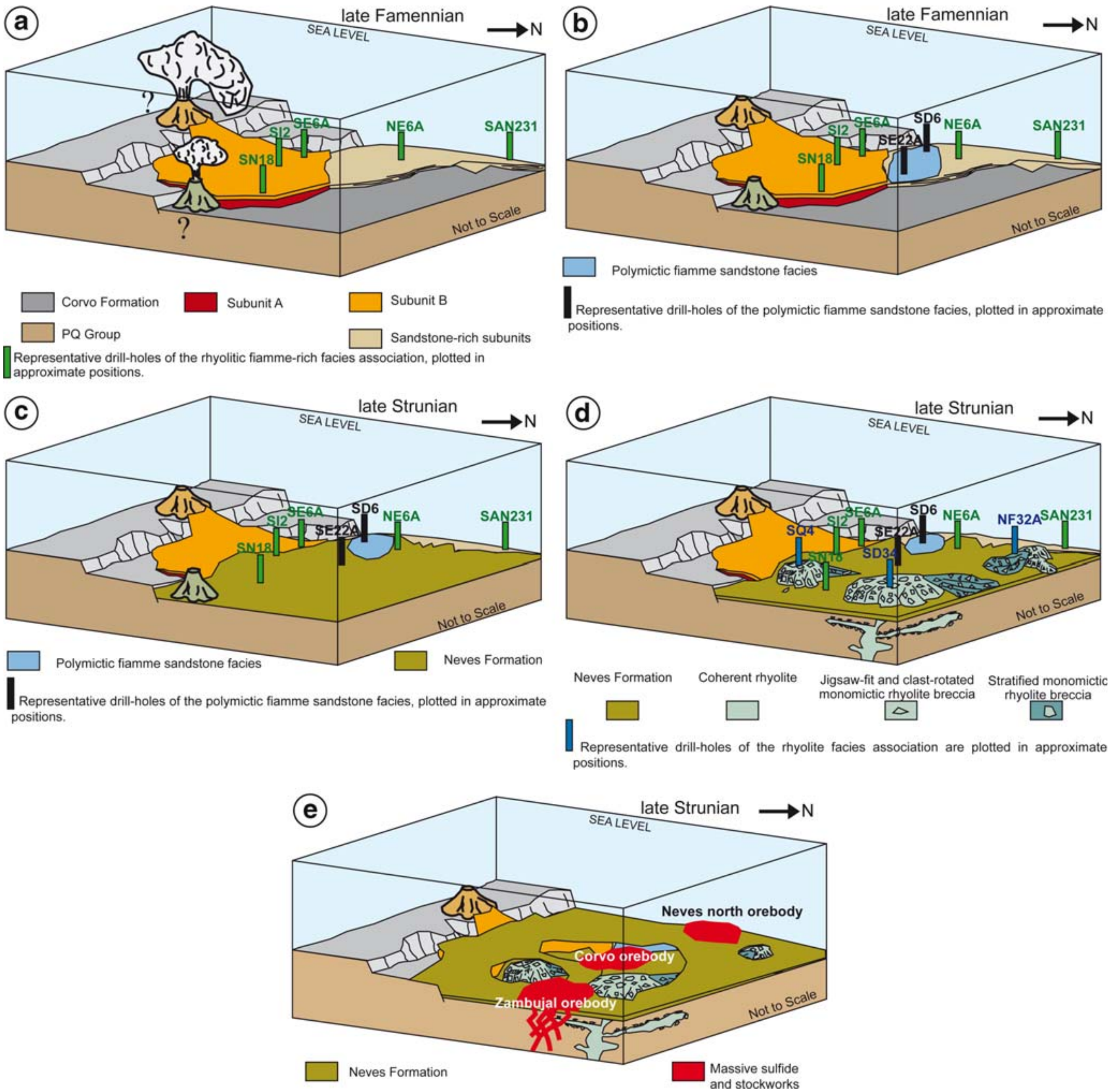

Fig. 12 **a** Schematic diagram representing the Neves Corvo depositional basin during the late Famennian. The rhyolitic fiamme-rich facies association originated from one or more vents with uncertain but possibly intrabasinal location. The relative positions of drill-holes that intersect the rhyolitic fiamme-rich facies association are also shown. **b** Schematic diagram representing the Neves Corvo depositional basin during the late Famennian showing the location of the polymictic fiamme sandstone facies. The relative positions of drill-holes that intersect the polymictic fiamme sandstone facies are also shown. **c** Schematic diagram representing the Neves Corvo depositional basin during the late Strunian. Drill-hole SD6 intersected an interval of the polymictic fiamme sandstone facies that is late Strunian. **d** Schematic diagram of the Neves Corvo depositional basin during the late Strunian representing the emplacement of rhyolite lava (rhyolite facies association). The relative positions of drill-holes that intersect the rhyolite facies association are also shown. The rhyolite lava or domes are shown only near the drill-holes but may be more extensive. **e** Schematic diagram of the Neves Corvo depositional basin during the late Strunian representing the emplacement of the massive sulfide ore bodies

eruption-fed gravity-current deposits (subunits A and B; Fig. 12a). Both subunits are coarsest in the southern part of the Neves Corvo Mine area and become finer grained and thinner towards the north and south. Hence, both gravity currents were most probably sourced from one or more vents in the southern part of the Neves Corvo area.

The polymictic fiamme sandstone facies is compositionally distinct from and younger than the fiamme-crystal sandstone facies in the lower volcanic sequence. This facies occurs either in late Fammenian or late Strunian mudstone and predates the ore-hosting intermediate volcanic sequence (Fig. 12b,c). The polymictic fiamme sandstone facies could be a relatively distal facies generated from explosive eruptions at vents with uncertain location. Alternatively, this facies may have formed by resedimentation of previously deposited, unconsolidated pyroclastic debris. More data on the spatial distribution and lateral variations of this facies are required to discriminate between primary and resedimented pyroclastic origins.

Early Strunian

Early Strunian strata are absent in the Neves Corvo area (Oliveira et al. 2004). According to Oliveira et al. (2004), this stratigraphic hiatus (~1 million years) may reflect local tectonic activity perturbing the sedimentation in the Neves Corvo area, as the hiatus is not recognized in the VSC elsewhere in the IPB.

Late Strunian volcanism

The gray to black mudstone of the Neves Formation was deposited in the late Strunian and is interbedded with one relatively thin (approximately 25 m thick) interval of polymictic fiamme sandstone (Fig. 12c). However, almost all the late Strunian volcanism in the Neves Corvo area is represented by the intermediate volcanic sequence. This unit was generated by purely effusive activity and consists of rhyolitic lava (rhyolite facies association; Fig. 12d).

The rhyolitic lava varies in thickness from 85 to 135 m (true thickness) in most of the Neves Corvo area. However, its thickness reaches approximately 250 m (true thickness) about 2.5 km to the SE of the Zambujal ore body (intersected in drill-hole MB1; Fig. 2). This location may have been closer to the source vent, or else, a separate dome or lava. The rhyolite facies association comprises coherent rhyolite lobes and rhyolitic hyaloclastite, a combination that is typical of felsic submarine lavas and domes (e.g., Yamagishi and Dimroth 1985). The rhyolitic lava overlies either the mudstone of the Neves Formation or the rhyolitic fiamme-rich facies association, indicating that the basin was floored by both units when the lavas were emplaced. In drill-hole NF32A (Figs. 2 and 9), two intersections of the rhyolite facies association are interbedded within the same unfaulted mudstone interval, suggesting that at least two separate effusive events may have taken place over that period of mud deposition.

The Neves Corvo rhyolitic lava has thicknesses and facies characteristics similar to other submarine felsic lavas in old and young submarine volcanic successions (e.g., Pichler 1965; De Rosen-Spence et al. 1980; Yamagishi and Dimroth 1985; Kano et al. 1991; Scutter et al. 1998; Doyle and McPhie 2000). Although source vents could not be precisely located, they were most probably intrabasinal seafloor vents situated within the Neves Corvo area because submarine felsic lavas typically extend no more than a few kilometers from source (e.g., De Rosen-Spence et al. 1980; McPhie et al. 1993). The massive sulfide ore bodies are the same age as, and some directly overlie, the rhyolite facies association, which shows pronounced ore-related hydrothermal alteration and widespread replacement textures (Fig. 12e; Relvas et al. 2006a). Hence, the Neves Corvo massive sulfide ore probably formed during the final stages of, or shortly after, the emplacement of the rhyolite lava.

Early Visean volcanism

Tournaisian strata are absent in the Neves Corvo area. The significance of this stratigraphic hiatus (~14 million years) is still poorly understood (Oliveira et al. 2004).

Sedimentation was restored during the lower early Visean, with deposition of mud of the Graça Formation. This formation encloses the lower early Visean dacitic jigsaw-fit breccia facies intersected only in drill-hole MB1 and has uncertain mode of emplacement. Other minor records of early Visean volcanism have been reported by Oliveira et al. (2004) in the Neves Corvo Mine area. These thin and laterally restricted intervals occur above the massive sulfide ore bodies and were not affected by ore-related hydrothermal alteration.

Younger early Visean strata are also absent in Neves Corvo (Oliveira et al. 2004), corresponding to a stratigraphic hiatus of approximately two million years. During the middle and late Visean, deposition of fine-grained sediments formed the Grandaços, "Borra de Vinho", Godinho, and Brancanes Formations (Oliveira et al. 2004).

Conclusions

The volcanic and sedimentary succession that hosts the Neves Corvo massive sulfide deposit was constructed on dark gray and black mud of late Famennian age immediately overlying the Phyllite–Quartzite Group. The depositional environment was submarine and below wave base. Palynomorph associations in black mudstone interbedded with volcanic units in the VSC at Neves Corvo indicate a late Famennian to mid-late Visean age for the host succession overall. This range corresponds to a duration in the order of approximately 35 million years for the entire volcanic and sedimentary succession of Neves Corvo. The three volcanic sequences (lower, intermediate, and upper) span approximately 22 million years. However, the intermediate volcanic sequence (rhyolite facies association), which is associated with the massive sulfide ore bodies, was probably produced by much shorter-lived volcanic events, since it occurs within the Neves Formation of late Strunian age (Strunian time span is approximately 360.7 to 361.5 Ma; Kaufmann 2006).

The volcanic facies and facies associations at Neves Corvo comprise the products of explosive and effusive eruptions. The first volcanic event in the Neves Corvo area occurred in the late Famennian (Late Devonian) and was explosive, generating water-supported, rhyolitic pumiceous pyroclastic gravity flows that deposited two very thick, graded units of pumice (now fiamme) breccia (lower volcanic sequence). The gravity flows were sourced from one or more submarine vents. The two fiamme breccia subunits lack evidence of hot emplacement. Relatively small and/or distant explosive eruptions persisted until the late Strunian, forming thin pumice- and crystal-rich units (polymictic fiamme sandstone facies) interbedded with mudstone.

During the late Strunian, a second major volcanic event generated rhyolitic lava (intermediate volcanic sequence) erupted from submarine intrabasinal vents. The lava underwent intense quench fragmentation and consists mainly of in situ hyaloclastite. The rhyolitic lava forms the immediate footwall to the Neves Corvo massive sulfide ore bodies, which are also late Strunian in age (Oliveira et al. 2004).

The third volcanic event occurred in the early Visean (upper volcanic sequence) and produced minor dacitic volcanic units that were not affected by the ore-related hydrothermal alteration.

Although the VSC at Neves Corvo includes three distinct volcanic sequences, one of which is closely linked to the ore bodies, it is largely composed of sedimentary units. This dominance of sedimentary facies is typical of the VSC throughout the IPB, even in mineralized areas, and contrasts with the volcanic-dominated nature of many other VHMS provinces worldwide.

Acknowledgments The work of CJPR was supported by a PhD scholarship from Fundação para a Ciência e Tecnologia, Portugal (POCI2010 and FSE). The CODES ARC Centre of Excellence in Ore Deposits at the University of Tasmania, the Centro de Recursos Minerais, Mineralogia e Cristalografia (CREMINER)/GeoFCUL at the University of Lisbon, and the Departamento de Prospecção de Minérios Metálicos of INETI (ex-IGM) hosted and supported the PhD program of CJPR. Professors Jocelyn McPhie and Jorge Relvas are acknowledged for their support and supervision of the PhD. The study was funded by the research project ARCHYMEDES I (Fundação para a Ciência e Tecnologia-POCTI/CTA/41393/2001). SOMINCOR is gratefully acknowledged for providing access to the drill core and for logistical support during field work. V. Oliveira, J. Matos, D. Rosa, P. Caetano, G. Barriga and F. Barriga are thanked for sharing with us their thoughts and profound knowledge of the IPB and Neves Corvo geology.

References

Allen RL, Weihed P, Svenson S (1996) Setting of Zn–Cu–Au–Ag massive sulfide deposits in the evolution and facies architecture of a 1.9 Ga marine volcanic arc, Skellefte District, Sweden. Econ Geol 91:1022–1053

Barrie T, Amelin Y, Pascual E (2002) U–Pb geochronology of VMS mineralisation in the Iberian Pyrite Belt. Miner Depos 37:684–703

Boulter CA (1993a) Comparison of Rio Tinto, Spain, and Guaymas Basin, Gulf of California: an explanation of a supergiant massive sulfide deposit in an ancient sill-sediment complex. Geology 21:801–804

Boulter CA (1993b) High-level peperitic sills at Rio Tinto, Spain: implications for stratigraphy and mineralization. Trans Inst Min Metall (Section B: Applied Earth Science) 102:B30–B38

Boulter CA (1996) Extensional tectonics and magmatism as drivers of convection leading to Iberian Pyrite Belt massive sulphide deposits. J Geol Soc (Lond) 153:181–184

Boulter CA (2002) It's a volcanic centre, Jim, but not as we know it. Trans Inst Min Metall (Section B: Applied Earth Science) 110: B208–B209

Boulter CA, Soriano C, Zimman P (2001) The Iberian Pyrite Belt: a mineralized system dismembered by voluminous high-level sills. Terra Nova 13:99–104

Boulter CA, Hopkinson LJ, Ineson MG, Brockwell JS (2004) Provenance and geochemistry of sedimentary components in the Volcano-Sedimentary Complex, Iberian Pyrite Belt: discrimination between the sill-sediment-complex and volcanic-pile models. J Geol Soc (Lond) 161:103–115

Carvalho P, Ferreira A (1994) Geologia de Neves Corvo: estado actual do conhecimento. In: II Simp Sulfuretos Polimetálicos da Faixa Piritosa Ibérica, Évora. Portugal Mineral 36:7–8

Carvalho D, Barriga FJAS, Munhá J (1999) Bimodal-siliciclastic systems—the case of the Iberian Pyrite Belt. Rev Econ Geol 8:375–408

De Rosen-Spence AF, Provost G, Dimroth E, Gochnauer K, Owen V (1980) Archaean subaqueous felsic flows, Rouyn-Noranda, Quebec, Canada and their Quaternary equivalents. Precambrian Res 12:43–77

Donaire T, Sáez R, Pascual E (2002) Rhyolitic globular peperites from the Aznalcóllar mining district (Iberian Pyrite Belt, Spain): physical and chemical controls. J Volcanol Geotherm Res 114:119–128

Doyle MG, McPhie J (2000) Facies architecture of a silicic intrusion-dominated volcanic centre at Highway-Reward, Queensland, Australia. J Volcanol Geoterm Res 99:79–96

Gibson HL, Watkinson DH (1990) Volcanogenis massive sulphide deposits of the Noranda Cauldron and Shield Volcano, Quebec. The Northwestern Quebec Polymetallic Belt, Canadian Institute Mining Metallurgy, special volume 43:119–132

Gifkins CC, McPhie J, Allen RL (2002) Pumiceous rhyolitic peperite in ancient submarine volcanic successions. J Volcanol Geoterm Res 114:181–203

Kano K, Takeuchi K, Yamamoto T, Hoshizumi H (1991) Subaqueous rhyolite block lavas in the Miocene Ushikiri Formation, Shimane Peninsula, SW Japan. J Volcanol Geoterm Res 46:241–253

Kano K, Yamamoto T, Ono K (1996) Subaqueous eruption and emplacement of the Shinjima Pumice, Shinjima (Moeshima) Island, Kagoshima Bay, SW Japan. J Volcanol Geoterm Res 71:187–206

Kaufmann B (2006) Calibrating the Devonian Time Scale: a synthesis of U-Pb ID-TIMS ages and conodont stratigraphy. Earth Scie Rev 76:175–190

Kokelaar P (1986) Magma-water interactions in subaqueous and emergent basaltic volcanism. Bull Volcanol 48:275–289

Korn D (1997) The Palaeozoic ammonoids of the South Portuguese zone. Mem Inst Geol Min Portugal 33:1–131

Leistel JM, Marcoux E, Thiéblemont E, Quesada C, Sánchez A, Almodovar GR, Pascual E, Sáez R (1998) The volcanic-hosted massive sulphide deposits of the Iberian pyrite belt. Miner Depos 33:2–30

Lowe DR (1982) Sediment gravity flows: II Depositional models with special reference to the deposits of high-density turbidity currents. J Sediment Petrol 52:279–297

McPhie J, Allen RL (1992) Facies architecture of mineralized submarine volcanic sequences: Cambrian Mount Read Volcanics, western Tasmania. Econ Geol 87:587–596

McPhie J, Allen RL (2003) Submarine, silicic, syn-eruptive pyroclastic units in the Mount Read Volcanics, western Tasmania: influences of vent setting and proximity on lithofacies characteristics. In: White JL, Smellie JL, Clague DA (eds) Explosive subaqueous volcanism. Geophysical Monograph Series 140, pp 245–258

McPhie J, Doyle MG, Allen RL (1993) Volcanic textures: a guide to the interpretation of textures in volcanic rocks. University of Tasmania, CODES, Hobart 198 pp

Mirão JAP, Barriga FJAS, Noiva P, Ferreira A (1997) Chemical sediments in the Neves Corvo Mine: the JC unit. Neves Corvo Field Conference Abstracts, Lisbon, 111

Munhá JM, Pacheco N, Beliz A, Relvas JMRS, Hodder RW (1997) Physical and geochemical characterization of the Neves Corvo felsic volcanism. Soc Econ Geol Neves Corvo Field Conference Abstract 89

Munhá J, Relvas JMRS, Barriga FJAS, Conceição P, Jorge RCGS, Mathur R, Ruiz J, Tassinari CCG (2005) Os isotopes systematics in the Iberian Pyrite Belt. In: Mao J, Bierlein FP (eds) Mineral deposit research: meeting the global challenge, v. 1. Proceedings of the 8th Biennial SGA Meeting, Beijing, China, August 2005. Springer, Berlin, Germany, pp 663–666

Oliveira JT (1990) Stratigraphy and synsedimentary tectonism. In: Dallmeyer RD, Martinez Garcia E (eds) Pre-mesozoic geology of Iberia. Springer, Berlin, pp 334–347

Oliveira JT, Pereira Z, Carvalho P, Pacheco N, Korn D (2004) Stratigraphy of the tectonically imbricated lithological succession of the Neves Corvo Mine area, IPB, Portugal. Miner Depos 39:422–436

Pereira Z, Pacheco N, Oliveira JT (2003) A case of applied palynology: dating the lithological succession of the Neves-Corvo Mine, Iberian Pyrite Belt, Portugal. In: Wong TE (ed) Proceedings of the XVth International Congress on Carboniferous and Permian Stratigraphy. R. D. Academy Arts and Sciences, Utrecht, The Netherlands, pp 345–354

Pichler H (1965) Acid hyaloclastites. Bull Volcanol 28:293–310

Quesada C (1998) A reappraisal of the structure of the Spanish segment of the Iberian Pyrite Belt. Miner Depos 33:31–44

Relvas JMRS (2000) Geology and metallogenesis at the Neves Corvo deposit, Portugal. Ph.D. thesis, Universidade de Lisboa, 319 pp

Relvas JMRS, Tassinari CG, Munhá J, Barriga FJAS (2001) Multiple sources for ore-forming fluids in the Neves Corvo VMS deposit of the Iberian Pyrite belt (Portugal): strontium, neodymium and lead isotope evidence. Miner Depos 36:416–427

Relvas JMRS, Barriga FJAS, Pinto A, Ferreira A, Pacheco N, Noiva PC, Barriga G, Baptista R, Carvalho D, Oliveira V, Munhá J, Hutchinson RW (2002) The Neves-Corvo deposit, Iberian pyrite belt, Portugal: Impacts and future, 25 years after the discovery. Society of Economic Geologists Special Publication 9, pp 155–176

Relvas JMRS, Barriga FJAS, Ferreira A, Noiva PC, Pacheco N, Barriga G (2006a) Hydrothermal alteration and mineralization in the Neves-Corvo volcanic-hostemassive sulfide deposit, Portugal. I. Geology, mineralogy, and geochemistry. Econ Geol 101:753–790

Relvas JMRS, Barriga FJAS, Longstaffe F (2006b) Hydrothermal alteration and mineralization in the Neves-Corvo volcanic-hosted massive sulfide deposit, Portugal. II. Oxygen, hydrogen, and carbon isotopes. Econ Geol 101:791–804

Rogers N, van Staal CR, McNicoll V, Thériault R (2003) Volcanology and tectonic setting of the northern Bathurst Mining Camp Part 1. Extension and rifting of the Popelogan arc. In: Goodfellow WD, McCutcheon SR, Peter J (eds) Massive sulphide deposits in the Bathurst mining camp, New Brunswick, and Northern Maine. Econ Geol Monogr 11:157–179

Rosa CJP (2007) Facies architecture of the Volcanic Sedimentary Complex of the Iberian Pyrite Belt, Portugal and Spain. Ph.D. thesis, University of Tasmania, 357 pp

Rosa CPJ, McPhie J, Relvas JMRS, Pereira Z, Pacheco N (2005) Felsic pyroclastic and effusive volcanic facies hosting the Neves-Corvo massive sulfide deposit, Iberian Pyrite Belt, Portugal. In: Mao J, Bierlein FP (eds) Mineral deposit research: meeting the global challenge, v.1, Proceedings of the 8th Biennial SGA Meeting, Beijing, China, August 2005. Springer, Berlin, Germany, pp 691–694

Scutter CR, Cas RAF, Moore CL, De Rita D (1998) Facies architecture and origin of a submarine rhyolitic lava flow-dome complex, Ponza, Italy. J Geophys Res 103:27551–27566

Silva JB, Oliveira JT, Ribeiro A (1990) Structural outline of the South Portuguese zone. In: Dallmeyer RD, Martinez Garcia E (eds) Pre-mesozoic geology of Iberia. Springer, Berlin, pp 348–362

Soriano C, Casas JM (2002) Variscan tectonics in the Iberian Pyrite Belt, South Portuguese zone. Int J Earth Sci 91:882–896

Soriano C, Marti J (1999) Facies analysis of volcano-sedimentary successions hosting massive sulfide deposits in the Iberian Pyrite Belt, Spain. Econ Geol 94:867–882

Thiéblemont D, Pascual E, Stein G (1998) Magmatism in the Iberian Pyrite Belt: petrological constraints on a metallogenetic model. Miner Depos 33:98–110

Tornos F (2006) Environment of formation and styles of volcanogenic massive sulfides: the Iberian pyrite belt. Ore Geol Rev 28:259–307

Tornos F, Casquet C, Relvas JMRS (2005) Transpressional tectonics, lower crust decoupling and intrusion of deep mafic sills: a model for the unusual metallogenesis of SW Iberia. Ore Geol Rev 27:133–163

Valenzuela A, Donaire T, Pascual E (2002) Secuencia de facies volcanicas en el area del rio Odiel (Faja Piritica Iberica, España). Geogaceta 32:131–134

Yamagishi H (1987) Studies on the Neogene subaqueous lavas and hyaloclastites in southwest Hokkaido. Report of the Geological Survey of Hokkaido 59, pp 55–117

Yamagishi H, Dimroth E (1985) A comparison of Miocene and Archean rhyolite hyaloclastites: evidence for a hot and fluid rhyolite lava. J Volcanol Geotherm Res 23:337–355